Available online at www.sciencedirect.com
SCIENCE DIRECT
Optics Communications 263 (2006) 147–151
OPTICS COMMUNICATIONS
www.elsevier.com/locate/optcom

Spherical aberration correction system using an adaptive optics deformable mirror

M. Schwertner [a,*], M.J. Booth [a], T. Tanaka [b,1], T. Wilson [a], S. Kawata [b,1]

[a] Department of Engineering Science, University of Oxford, Parks Road, Oxford OX1 3PJ, United Kingdom
[b] Nanophotonics Laboratory, RIKEN, 2-1, Hirosawa, Wako, Saitama 351 0198, Japan

Received 9 September 2005; received in revised form 12 January 2006; accepted 14 January 2006

Abstract

A deformable membrane mirror is often used in closed loop adaptive optics systems to correct for aberrations and improve image quality. In certain applications, the correction of only one type of aberration is sufficient, the calibration procedure of the mirror can be simplified and the control scheme can be reduced to a fast feed forward system. For these cases we developed a procedure that is easy to implement, accurate and delivers a large correction range. An application example is the writing and readout of three-dimensional optical memory. Here the spherical aberration component is dominant and can be inferred from the focussing depth. We describe the principle of the new calibration and feed forward control scheme and give experimental results.

1. Introduction

In this article we will describe a method whereby a deformable mirror (DM) can be controlled so as to produce varying amounts of primary spherical aberration accurately over a large range. In certain applications only one type of aberration dominates—first-order spherical aberration. It has been shown that focusing through a refractive index mismatch introduces a spherical aberration component that depends linearly on focusing depth [1,2]. For example, this is the case in 3D optical memory applications where dry lenses are used to focus into a recording medium of high refractive index.

Adaptive optics [3] is a technique that allows dynamic correction of aberrations. It was originally developed for astronomy [4] but there are also applications in microscopy [5], the writing of 3D optical bit memory [6] and photo-fabrication [7]. As an active correction element, a micromachined DM [8] can be used to modify the phase of the beam. This device is attractive for many applications since it has a very good light efficiency. Usually, an adaptive optics system operates in closed loop mode, where an aberration sensor (for example a Shack Hartmann sensor [9] or a modal wavefront sensor [10,11]) is combined with the active correction device in a feedback loop. Based upon the measurement from the wavefront sensor, the aberration correction settings are updated and optimised continuously. Such adaptive optics schemes are useful for the correction of randomly varying aberrations.

However, when material parameters and the focusing depth are known, the adaptive optics system can be simplified. We can build an open loop adaptive optics system without a wavefront sensing element. This element would be obsolete if we had an active correction device that could produce a specified amount of spherical aberration. Such a scheme is sometimes referred to as feed forward control.

2. Deformable mirror characteristics

The DM we use in our experiments is based on a continuous, aluminum coated flexible membrane that is suspended

* Corresponding author. Tel.: +44 1865273097; fax: +44 1865273905.
E-mail addresses: Michael.Schwertner@eng.ox.ac.uk (M. Schwertner), Tony.Wilson@eng.ox.ac.uk (T. Wilson), kawata@riken.jp (S. Kawata).
[1] Tel.: +81 48 462 1111.

0030-4018/$ - see front matter © 2006 Elsevier B.V. All rights reserved.
doi:10.1016/j.optcom.2006.01.026

over a hexagonal array of 37 electrostatic actuators (OKO Technologies, The Netherlands) [8]. The control method described here is not limited to this specific device; there are several types of deformable mirrors commercially available that have similar properties.

The differences between the potential of the membrane and the electrodes creates forces that define the shape of the membrane. We describe the state of the mirror by the set of control signals $[c_i]$ where $1 \leqslant i \leqslant N$ and N denotes the number of actuators. Since the local deflection of the membrane is approximately proportional to the square of the applied voltage, it is common to represent the mirror state by linearised control signals that are directly related to the membrane deflection. As a consequence the actual voltages sent to the mirror are proportional to the square root of the control signals. The mirror is usually biased with a constant voltage in order to permit displacement both towards and away from the electrodes.

The DM device itself introduces an initial aberration, mainly astigmatism, that needs active correction. Also the actuators show slightly nonlinear response and crosstalk [12]. The actual surface shapes that can be obtained are restricted by the properties of the membrane. An initial calibration procedure is therefore required to account for the specific properties of the DM device and acquire the relationship between the mirror shape and the control parameters.

3. Calibration procedure

A phase function ψ representing the wavefront can be described by its aberration mode content. It is common to use the Zernike polynomials $Z_i(r,\theta)$ [13] for this purpose. They are a set of orthogonal functions over the unit circle. Phase functions defined over the unit circle can be described by their Zernike mode amplitudes M_i given by

$$M_i = \frac{1}{\pi}\int_0^1 \int_0^{2\pi} \psi(r,\theta,[c_i]) Z_i(r,\theta) r \,\mathrm{d}\theta \,\mathrm{d}r. \tag{1}$$

Here r is the radius within the pupil and is normalised to unity, θ is the angular coordinate and $[c_i]$ again refers to the set of control signals that determine the shape of the mirror. First-order spherical aberration is represented by the Zernike polynomial Z_{11}:

$$Z_{11}(r) = \sqrt{5}(6r^4 - 6r^2 + 1). \tag{2}$$

This also defines our normalisation: the wavefront $\psi(r,\theta,[c_i])$ contains M_{11} Zernike units of first-order spherical aberration when we use Eq. (1) in combination with (2). The definition of other Zernike coefficients and the indexing scheme we use are listed in [11,13].

Our goal is now to develop a control method for the DM that allows generation of a wavefront phase $\psi(r,\theta,[c_i])$ with a specific spherical aberration amplitude M_{11}. Hence we wish to produce

$$\psi(r,\theta,[c_i]) = M_{11} Z_{11}, \tag{3}$$

where all the other aberration components are minimised ($M_i \approx 0$ for $i \neq 11$). In order to achieve that we propose to:

(1) Obtain a simplified linear control model of the mirror based on the measurement of local deflection.
(2) Optimise wavefront quality for a given set of Zernike mode amplitudes M_{11} in an iterative manner by means of wavefront measurements and application of the simplified linear control model.
(3) Create a look-up table (LUT) by means of interpolation to give fast access to the DM control signals required to provide varying amounts of spherical aberration.

In the following, the above steps will be explained; we start with the simplified linear control model. The aim is to provide an intermediate control scheme for the mirror that is easy to implement but sufficiently accurate to deliver good convergence of the iterative algorithm for wavefront error optimisation. If r_k and θ_k are the coordinates of the center of the actuator number k we define the local deflection d_k as the difference in radians between the phase function at the position of the actuator k and the average of the phase function over the active DM area:

$$d_k(\psi(r,\theta,[c_i])) = \psi(r_k,\theta_k,[c_i]) - \frac{1}{\pi}\int_0^{2\pi}\int_0^1 \psi(r,\theta,[c_i]) r \,\mathrm{d}r \,\mathrm{d}\theta. \tag{4}$$

Therefore d_k represents the local deflection at the location of actuator k in response to the set of applied control signals, $[c_i]$. Now the linear dependence of the deflection d_k on the control signal c_k for each actuator number k is extracted from a linear least squares fit of the data:

$$d_k(c_{i=k}) = s_k c_{i=k} + o_k. \tag{5}$$

To acquire one slope value s_k in (5) only $c_{i=k}$ is varied while all other control signals c_i for $i \neq k$ are set to the constant bias value. In our notation c_i refers to a single control signal while $[c_i]$ always refers to the whole set of signals. The values s_k indicate the sensitivity of the local deflection to the corresponding control signal and o_k is a constant offset term for each actuator k. The sensitivity of the outer electrodes is significantly smaller because the movement of the membrane is restricted in the vicinity of the membrane edge. Good linearity of the deflection response was observed but crosstalk up to 50% between local deflections of neighboring actuators was found. This is not a problem since the values of s_k are used in the intermediate iterative algorithm only. The crosstalk influences the convergence speed but not the accuracy, which is a strength of the proposed approach. For each iteration procedure the spherical aberration target wavefront is denoted by $\psi_T(r,\theta)$. It can be generated from (2). The change Δc_k for each control signal per iteration step is then

$$\Delta c_k = \frac{\alpha}{s_k} d_k(\psi_T(r,\theta) - \psi(r,\theta,[c_i])), \tag{6}$$

where α is a constant parameter that determines the convergence properties of the iteration against the target shape of the wavefront. The iteration is repeated until the spherical wavefront quality is a stable maximised value. It was found experimentally that a value in the range of $\alpha = 0.3 \pm 0.1$ delivered good convergence, typically achieved after 4–8 iterations depending on the difference between the target wavefront and the initial state of the DM. The iteration is robust and not very sensitive in respect to the choice of α. Too small values lead to slow convergence while too large values can cause oscillations of the solution due to over-correction. The optimum value also depends on the crosstalk between actuators, i.e. the specific mirror device. It should be mentioned that the speed of the convergence and hence the adjustment of α is not critical since the iteration occurs only during the initial calibration process. As a measure for the wavefront quality and a criterion for the termination of the iteration the Strehl ratio of the residual wavefront error is used as explained in Section 4.

In the final step of the calibration process a look-up table (LUT) is generated. The intermediate iteration procedures finish with several optimised sets of control voltages that all correspond to different values of the Zernike amplitude M_{11}. The data can be regarded as a set of functions, describing the control signals for the mirror at each discrete value of M_{11} that was used in the iteration. We use cubic spline interpolation to create a LUT for the intermediate values. In our case this LUT has the requested target amplitude of Zernike mode 11 (at a quantisation of 1/100 Zernike mode units) as input and delivers all control signals for the mirror accurately and quickly. This is relevant for the implementation of fast open loop correction systems.

It is important to mention that, during the iteration process, saturation of some of the mirror actuators may occur. The maximum positive value of the Zernike polynomial Z_{11} is greater in magnitude than the largest negative value. From Eq. (2) we see that Z_{11} covers the range of $\sqrt{5}(-0.5, 1.0)$ radians. Obviously, the positive portion of Z_{11} would saturate the mirror actuators first. However, to solve this problem, a variable, uniform offset of the control signals is incorporated into the iteration procedure. We can therefore extend the useful range before saturation occurs. This also implies that the functions contained in the LUT are nonlinear. This possibility is an advantage of the new method and cannot be achieved with other approaches in the literature that are based on a linear control matrix.

4. Experimental set-up and wavefront measurement

For the calibration of the DM we built an interferometer as shown in Fig. 1. All the measurements utilised light from a 632.8 nm HeNe laser; the DM has a nominal diameter of 15 mm but only 70% of this nominal diameter is used as the active area. This sub-aperture of 10.5 mm fully covers the actuator structure underneath the membrane.

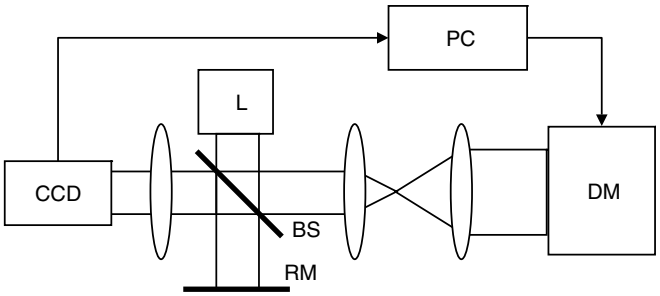

Fig. 1. Set-up for the calibration of the deformable mirror. The components are denoted as follows: L – laser, CCD – charge coupled device, PC – personal computer equipped with framegrabber, BS – beamsplitter, RM – flat reference mirror, DM – deformable mirror.

Note that the optical path difference introduced by the DM corresponds to twice the deflection of the membrane. In the normal mode of operation the DM is biased in order to allow positive and negative deflections with respect to the initial shape. This introduces an additional defocus which is compensated for by illuminating the DM with a slightly diverging wavefront.

After reflection from the DM the wavefront may be described by the complex function

$$P(r, \theta, [c_i]) = A(r, \theta) \exp(j\psi(r, \theta, [c_i])), \tag{7}$$

where $A(r, \theta)$ denotes the amplitude and $\psi(r, \theta, [c_i])$ the phase as before. The flat reference mirror in Fig. 1 is slightly tilted and the CCD records a fringe pattern interferogram. Using a combination of fringe pattern analysis [14] and phase unwrapping [15] the phase $\psi(r, \theta, [c_i])$ of the wavefront can be obtained from a single interferogram.

During the initial calibration of the DM we need to evaluate the wavefront quality. To do this we first obtain the spherical (M_{11}), tip (M_2) and tilt (M_3) coefficients from (1) and then calculate the residual wavefront error:

$$\psi_E(r, \theta) = \psi(r, \theta, [c_i]) - M_{11}Z_{11} - M_2Z_2 - M_3Z_3, \tag{8}$$

which is the measured wavefront where its first-order spherical, tip and tilt components have been removed. This also compensates for any residual tip or tilt the reference wavefront. For the calculation of the amplitudes M_2 and M_3 in (1) we used the definitions $Z_2 = 2r\cos\theta$ and $Z_3 = 2r\sin\theta$.

Now we can describe the quality of the generated wavefront using the Strehl ratio S_E of the residual wavefront error:

$$S_E = \frac{\left| \int_0^1 \int_0^{2\pi} A(r, \theta) \exp(j\psi_E(r, \theta)) r \, dr \, d\theta \right|^2}{\left(\int_0^1 \int_0^{2\pi} A(r, \theta) r \, dr \, d\theta \right)^2}. \tag{9}$$

This definition of the Strehl ratio is slightly different from [16] and takes into account the amplitude distribution of the wavefront, $A(r, \theta)$. For small wavefront errors the Strehl ratio is also related to the variance $\sigma^2(\psi_E)$ of the wavefront error via the Marechal approximation: $S_E = \exp[-\sigma^2(\psi_E)]$.

5. Results

In Fig. 2 the phase measurement process is illustrated with a wavefront that was created using the described iteration process. The dots indicate the electrode positions where the deflections are measured.

To verify our calibration procedure, a number of first-order spherical aberration wavefronts were created using the lookup table. The wavefront quality was analysed by interferometric measurements and Strehl ratio calculations. In Fig. 3 examples for the amplitudes $M_{11} = -2.0$, 0.0, 2.0 are displayed and Fig. 4 shows the Strehl ratios S_E of the wavefront error for several amplitudes. The wavefront error depends on the Zernike mode amplitude requested; better correction can be achieved for smaller amplitudes. The total correction range is also limited by the stroke of the actuators. An optical system is considered to be well corrected if the Strehl ratio is larger than 0.80. This corresponds to an RMS wavefront error of 0.47 rad or $\lambda/13$.

Another important parameter is the accuracy and linearity of the amplitude of the generated phase pattern. In Fig. 5 the measured spherical aberration component is plotted against the target amplitude that was requested from the LUT. Good linearity is observed and the RMS deviation from the requested value (straight line) was 0.028 Zernike units defined according to (2).

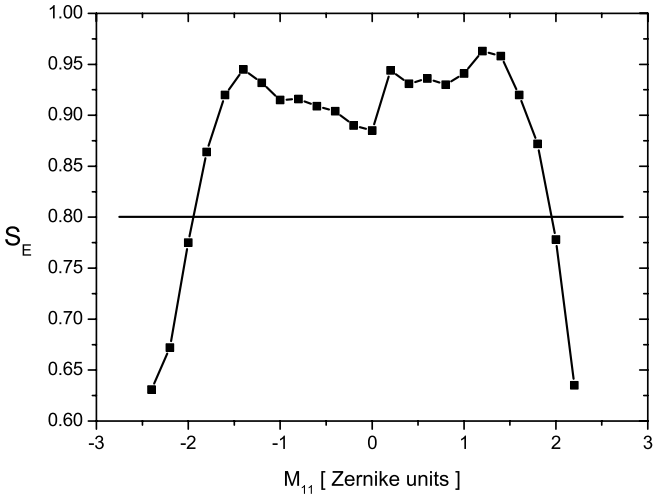

Fig. 4. The variation of S_E with the Zernike mode amplitude M_{11} of the phase pattern produced using the lookup table. An optical system with a Strehl ratio of 0.8 (horizontal line) is considered to be well corrected. Note that the Zernike mode amplitudes refer to the deformation of the wavefront after reflection, which is twice the deformation of the mirror. The same applies to Fig. 5.

6. Discussion and conclusion

We have presented a method for controlling a DM in order to provide first-order spherical aberration correction.

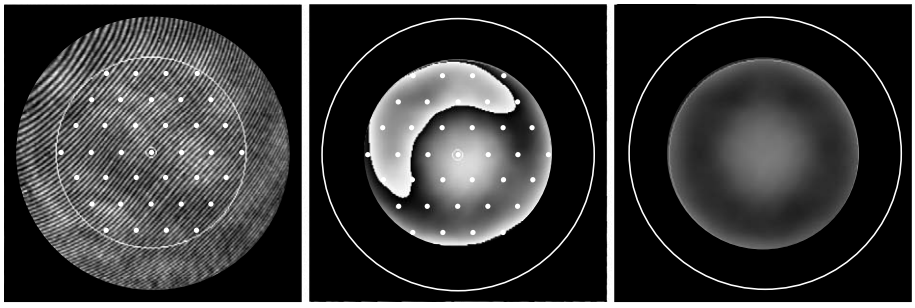

Fig. 2. Example wavefront for an iteration result: 1.5 units of Zernike mode number 11 (first-order spherical aberration). Left: interference fringe image. Middle: recovered wrapped phase function, black corresponds to 0 and white corresponds to 2π. A small superimposed tilt of the reference wavefront is visible. Right: unwrapped phase function, the tip and tilt components were removed. Note that the active area of the DM that is used for the phase modulation of beams is contained within the inner circle, the outer circle indicates the full aperture of the DM. The white dots show the actuator positions.

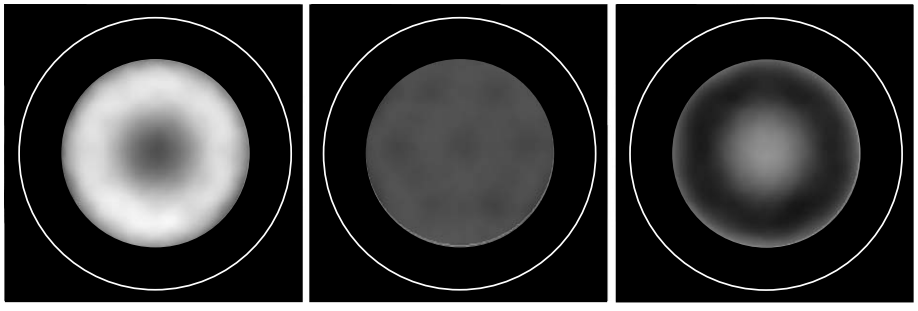

Fig. 3. Example wavefronts for the generation of Zernike mode number 11 (first-order spherical aberration) using the LUT as described in the text. From left to right, the Zernike mode amplitudes were −2.0, 0.0 and +2.0 Zernike mode units and S_E was 0.77, 0.88, and 0.76, respectively.

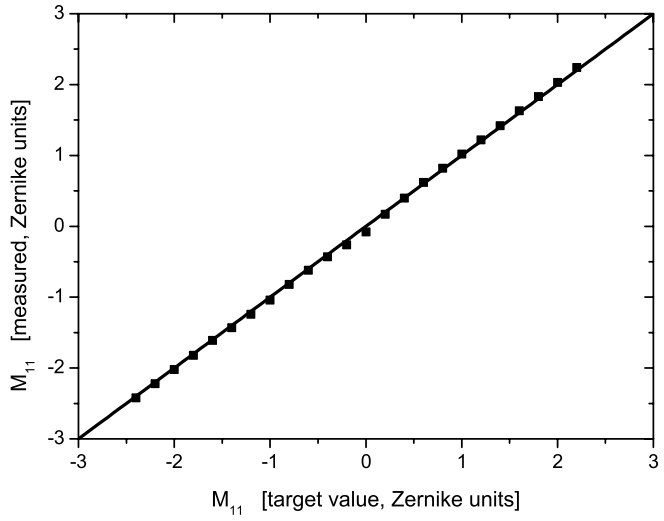

Fig. 5. Plot of the measured spherical aberration Zernike mode amplitude against the requested amplitude using the described lookup table in an open loop regime.

In the previous literature, other methods are described, for example [14,17,18]. However, they try to obtain a complete control model of the mirror for the correction of arbitrary aberrations. They also make the approximation that the mirror response is an exact superposition of individual actuator signals and assume the response is linear with respect to actuator signals. The method proposed here does not need to make these approximations, which allows improved accuracy. In addition, the described methods [14,17,18] define the mirror control signals with respect to a bias position, which is usually the middle of the actuator range. In the case of spherical aberration however, the Zernike polynomial is not symmetric about zero and asymmetric saturation of the actuators would limit the correction range of the DM for these methods. The iteration procedure we propose here uses a variable uniform offset of the control signals. Therefore, larger spherical mode amplitudes due to optimum use of the available actuator range of the DM can be achieved. In the experiment we measured a range of approximately ± 1.9 Zernike mode units of spherical aberration at a Strehl ratio of better than 0.8 for the residual wavefront error.

Note that the intermediate iterative scheme implemented for the creation of the LUT could also be used for a closed loop iterative adaptive optics system, although this was not the goal of this investigation.

We can conclude that this simplified calibration procedure is suitable for the construction of an open loop adaptive optics correction system for the correction of any type of aberration where the same wavefront pattern at different amplitudes is required. The method presented here delivers good performance in wavefront quality, a large correction range and is straightforward to implement.

Acknowledgements

We gratefully acknowledge support from the Japanese Society for the Promotion of Science, the Deutscher Akademischer Austauschdienst Germany and the Basic Technology initiative from the Research Councils UK for this work. MJB is a Royal Academy of Engineering/EPSRC Research Fellow.

References

[1] S. Hell, G. Reiner, C. Cremer, E. Stelzer, J. Microsc. 169 (3) (1993) 391.
[2] M. Booth, M. Neil, T. Wilson, J. Microsc. 192 (2) (1998) 90.
[3] R. Tyson, Principles of Adaptive Optics, Academic Press Inc., San Diego, CA, 1991.
[4] J.W. Hardy, Adaptive Optics for Astronomical Telescopes, Oxford University Press, 1998.
[5] M. Booth, M. Neil, R. Juškaitis, T. Wilson, Proc. Natl. Acad. Sci. 99 (2002) 5788.
[6] M.J. Booth, M. Schwertner, T. Wilson, M. Nakano, Y. Kawata, M. Nakabayashi, S. Miyata, Appl. Phys. Lett. 88 (2006) 031109.
[7] S. Kawata, H.-B. Sun, T. Tanaka, K. Takada, Nature 412 (2001) 697.
[8] G. Vdovin, P. Sarro, S. Middelhoek, J. Micromech. Microeng. 9 (2) (1999) R8.
[9] B. Platt, R. Shack, J. Refract. Surg. 17 (2001) 573.
[10] M.J. Booth, M.A.A. Neil, T. Wilson, J. Opt. Soc. Am. A 19 (10) (2002) 2112.
[11] M.A.A. Neil, M.J. Booth, T. Wilson, J. Opt. Soc. Am. A 17 (6) (2000) 1098.
[12] L. Zhu, P. Sun, D. Bartsch, W. Freeman, Y. Fainman, Appl. Opt. 38 (1) (1999) 168.
[13] M. Schwertner, M.J. Booth, M. Neil, T. Wilson, J. Microsc. 213 (1) (2004) 11.
[14] M. Booth, T. Wilson, H.-B. Sun, T. Ota, S. Kawata, Appl. Opt. 44 (24) (2005) 5131.
[15] D. Ghiglia, M. Pritt, Two Dimensional Phase Unwrapping; Theory, Algorithms and Software, Wiley, 1998.
[16] M. Born, E. Wolf, Principles of Optics, sixth ed., Pergamon Press, 1983.
[17] C. Paterson, I. Munro, J.C. Dainty, A low cost adaptive optics system using a membrane mirror, Opt. Express 6 (2000) 175.
[18] E. Fernandez, P. Artal, Membrane deformable mirror for adaptive optics: performance limits in visual optics, Opt. Express 11 (9) (2003) 1056.